

# TOWARDS AN AMPLITUDE ANALYSIS OF $\pi^+ \pi^-$ PRODUCTION. DATA AT 15 GeV/c

C.D. FROGGATT(\*)

## INTRODUCTION

We discuss a model amplitude analysis of the 15 GeV/c SLAC data on the process

$$\pi^- p \longrightarrow \pi^+ \pi^- n$$

at small momentum transfer squared  $t$  to the nucleon and for the dipion mass  $M_{\pi\pi}$  in the rho band ( $0.665 < M_{\pi\pi} < 0.865$  GeV)<sup>1)</sup>. A complete amplitude analysis (i.e., without any model assumptions) requires the use of a polarized target<sup>2),3)</sup>. However, within the present level of statistics for experiments on this process, models<sup>4),5)</sup> having a quite simple amplitude structure reproduce the available data at small  $t$  ( $|t| < 0.2$  GeV<sup>2</sup>), where pion exchange appears to be the dominant dynamical mechanism. Here we want to investigate how strongly the data support the general structure of the amplitudes implied by these models.

We present an amplitude analysis of the  $\pi^+ \pi^-$  production process, assuming (nucleon) spin and phase coherence for the unnatural parity exchange component of the production amplitudes<sup>6)</sup>. Such coherence follows strictly in any high energy model in which production occurs via elementary one pion exchange modified by absorption (OPEA). An example is the simplified absorption model

---

(\*) and D. Morgan, RHEL, Chilton, England.

of Williams <sup>4)</sup> to which the SLAC data have already been fitted <sup>7)</sup>. The present approach can be regarded as a generalization <sup>8)</sup>. Simple Regge models without absorption <sup>9)</sup> also satisfy this coherence condition. More sophisticated models violate the coherence assumption. In particular Reggeized absorption models entail departures from coherence mainly in the phase and we illustrate these effects in our discussion.

The assumption of coherence is more than sufficient to determine the amplitudes and leads to constraints between experimental quantities. It turns out that the data under discussion do not furnish a very stringent test of these constraints. Two alternative procedures are adopted to derive amplitudes, a  $t$  independent analysis (TIAA) in which amplitudes are obtained separately for each  $t$  value and a  $t$  dependent analysis (TDAA) in which the data at all  $t$  values are fitted to parametric forms embodying OPE and a smooth background. We make some remarks on the background amplitudes and the  $S$  wave production amplitudes obtained.

#### DESCRIPTION OF AMPLITUDE ANALYSIS AND RESULTS

We assume for the production amplitudes : (i) that only  $S$  and  $P$  wave dipion production need be considered, (ii) production goes entirely by  $s$  channel nucleon-helicity flip, (iii) amplitudes are all relatively real except for an over-all  $S$ - $P$  decay phase difference (independent of  $t$ ). In fact, assumptions (ii) and (iii) are only necessary for the unnatural parity exchange components. We comment on these assumptions below. Intensity components are conveniently expressed in terms of the amplitudes  $F_S^{(0)}$   $e^{i\Delta}$  for  $S$  wave production,  $F^{(0)}$  for longitudinal  $P$  wave, and  $F^{(+)}$  and  $F^{(-)}$  for transverse  $P$  wave production respectively via natural and unnatural parity exchange :

$$(\sigma_{00} - \sigma_{11}) \frac{d\sigma}{dt} = F^{(0)2} - \frac{1}{4} (F^{(+2)} + F^{(-2)}) \quad (1)$$

$$\rho_{1-1} \frac{d\sigma}{dt} = \frac{1}{4} (F^{(+)}{}^2 - F^{(-)}{}^2) \quad (2)$$

$$\text{Re } \rho_{10} \frac{d\sigma}{dt} = \frac{1}{2} F^{(0)} F^{(-)} \quad (3)$$

$$\begin{aligned} (\rho_{00} + 2\rho_{11} + \rho_{ss}) \frac{d\sigma}{dt} \equiv \frac{d\sigma}{dt} = & F^{(0)}{}^2 + F_s^{(0)}{}^2 + \\ & + \frac{1}{2} [F^{(+)}{}^2 + F^{(-)}{}^2] \end{aligned} \quad (4)$$

$$\text{Re } \rho_{00}^s \frac{d\sigma}{dt} = F_s^{(0)} F^{(0)} \cos \Delta_0 \quad (\Delta_0 = \Delta) \quad (5)$$

$$\text{Re } \rho_{10}^s \frac{d\sigma}{dt} = \frac{1}{2} F_s^{(0)} F^{(-)} \cos \Delta_1 \quad (\Delta_1 = \Delta) \quad (6)$$

We work in the high energy limit so that  $F^{(\pm)}$  corresponds to  $F^{m=1} \pm F^{m=-1}$ . Furthermore,  $t_{\min} = 0$  and the s-t helicity crossing matrix is respectively diagonal (antidiagonal) in nucleon spins for natural (unnatural) parity exchange.

(A) TIAA

The t independent amplitude analysis to be discussed was accomplished by solving Eqs. (1), (2) and (3) for  $F^{(0)}$ ,  $F^{(-)}$  and  $F^{(+)}$ , then (4) for  $F_s^{(0)}$ . Equations (5) and (6) were treated as constraints, the requirement being  $\cos \Delta_0 = \cos \Delta_1 = \text{const.}$  (independent of t). (Other procedures could be adopted.)

(B) TDAA

The  $t$  dependent amplitude analysis was in the main performed by fitting the experimental intensity components to the following forms of the  $t$  channel amplitudes (in  $\sqrt{\mu}b \text{ GeV}^{-1}$ ) :

$$F^{(0)} = C^{(0)} \exp(D^{(0)}t/\mu^2) \sqrt{-t}\mu/(t-\mu^2) \quad (7)$$

$$F^{(-)} = C \exp(D^{(-)}t/\mu^2) \quad (8)$$

$$F^{(+)} = C \exp(D^{(+)}t/\mu^2) \quad (9)$$

$$F_s^{(0)} = C_s^{(0)} \exp(D_s^{(0)}t/\mu^2) \sqrt{-t}\mu/(t-\mu^2) \quad (10)$$

The fitted parameters are  $C^{(0)}$ ,  $C$ ,  $C_s^{(0)}$ ,  $D^{(0)}$ ,  $D^{(-)}$ ,  $D^{(+)}$ ,  $D_s^{(0)}$  and  $\cos\Delta$ .

Procedures (A) and (B) [in the latter case with the formulae (7) to (10) cast in the appropriate frame using the crossing matrix] were applied to both the experimental  $t$  channel and  $s$  channel intensity components to ensure that no information was lost through binning of data in  $t$ . For the  $s$  channel TDAA fits, alternative forms allowing different exponential form factors for no flip and double flip were also tried but the fits were not as good and this was not pursued. Fits were made both to all six experimental quantities (1) to (6) given equal weights (6C Fits) and with (5) and (6) essentially decoupled (4C Fits) (contribution to  $\chi^2$  multiplied by 0.1). The errors on experimental quantities were naively assumed to be uncorrelated.

The results are displayed in the Table and Figs. 1 to 8. Figures 1 to 4 show the  $t$  channel amplitudes obtained by TDAA (full line) and TIAA (the points with errors) with the fit to Williams' model <sup>4)</sup> (dashed line) superimposed for comparison. Figure 5 is a plot of the  $\cos\Delta_0$  and  $\cos\Delta_1$  values derived using Eqs. (5) and (6) as constraints. It is immediately clear that the constraints are neither seen to be violated nor strikingly vindicated. They appear to be adequately satisfied <sup>10)</sup>. Figure 6 gives an example of  $s$  channel amplitudes, Fig. 7 shows an example of the fit to the differential cross-section  $d\sigma/dt$  and Fig. 8 shows fits to density matrix elements in both the  $t$  and  $s$  channels (note the shift to  $\sqrt{-t}$  plots in Figs. 7 and 8 -  $t$  is shown in units of  $\mu^2 = 0.02 \text{ GeV}^2$ ,  $\sqrt{-t}$  in units of  $\mu$ ).

Interesting aspects of the TDAA results are :

- (i) the over-all magnitude is satisfactory - the observed peak in  $d\sigma/dt$  is at around  $360 \mu\text{b GeV}^{-2}$  while OPE would give for the P wave alone about  $300 \mu\text{b GeV}^{-2}$  ( $0.665 < M_{\pi\pi} < 0.865$ ) ;
- (ii) the ratio of S to P wave production via OPE  $C_S^{(0)}/C^{(0)}$  is in accord with expectation -

$$C_S^{(0)}/C^{(0)} = A_S^{\pi\pi}/\sqrt{3} A_P^{\pi\pi} \approx \frac{2}{3\sqrt{3}} = 0.385$$

if  $A_P, A_S^{I=0}$  resonant and  $A_S^{I=2}$  negligible ;

- (iii) the exponents are all rather similar at around  $\exp(0.09 t)$  except for that corresponding to natural parity exchange which is less steep  $\sim \exp(0.07 t)$  ; this last may be indicative of natural parity Regge contributions (A2) ; the emergence of the above exponent for S wave production [corresponding to  $\exp(9t/(\text{GeV}^2))$  in the cross-section] is of interest in view of the non-attainment of the unitarity limit for the  $\pi\pi$  charge exchange cross-section inferred from high energy data on  $\pi^- p \rightarrow \pi^0 \pi^0 n$  <sup>11), 12)</sup> if the

exponential slope which best fits the data,  $\exp(7t)$  is used. An exponential slope  $\exp(9t)$  is still adequate and results in a  $\sigma_{\pi\pi}(\text{CEX})$  which does achieve the unitarity limit <sup>12</sup>).

Comparison of the TIAA and TDAA results (Figs. 1-4 and 6) are in general satisfactory, except for  $F^{(-)}$ ,  $F^{(+)}$  and  $F_s^{(0)}$  for  $|t| < 0.8 \mu^2$ . The anomalous behaviour of the TIAA results for those amplitudes can be traced to the experimental results for  $\text{Re } \mathcal{F}_{10}^J$  (Fig. 8) <sup>8),13)</sup>. Preliminary results from the high statistics CERN-Munich experiment at 17 GeV/c indicate a behaviour more in accord with our prediction <sup>14)</sup>.

## DISCUSSION

We briefly discuss the assumptions of our analysis, their consequences, their relation to other peoples' assumptions and the extent to which the present assumptions can be said to be upheld by the data. We also discuss our result on the amount of transverse production at  $t = 0$  (the size of the parameter <sup>15)</sup>  $\gamma_1^P$ , in the Table). We conclude with some comments on further details which are of interest in experiments of this type and a plea for polarization experiments.

First our assumptions. Our first assumption, only S and P wave production for  $M_{\pi\pi} \lesssim M_S$  is conventional, but will in future have to be abandoned to accommodate the CERN-Munich data ( $\langle Y_{30} \rangle \neq 0$ ,  $\langle Y_{31} \rangle \neq 0$  <sup>14)</sup>). Hopefully, the results on S and P wave amplitudes will not be too much disturbed. The key assumptions are (ii) and (iii), that the production amplitudes are all s channel nucleon helicity flip and are all relatively real - i.e., the assumption of spin and phase coherence. As stated earlier, this follows strictly at high energy if production is

governed by elementary OPEA. A consequence of such coherence is the simplification of the expressions for intensity components in terms of amplitudes which we have exploited, allowing the amplitudes to be solved for, with equations to spare (constraints). As already mentioned the constraints of Eqs. (5) and (6) are not strongly tested in the present data (Fig. 5).

The method of Schlein<sup>16),17)</sup> assumes phase coherence but not spin coherence. In contrast conventional absorbed Reggeism ( $\pi + A_2$  exchanges with  $\pi$  entirely,  $A_2$  predominantly nucleon helicity flip) would readily assimilate spin coherence as a good first approximation but disfavour the concept of phase coherence. It should be noted that the natural parity exchange amplitude only occurs in the form  $|F^+|^2$  in Eqs. (1) to (6). It follows that it is only the phase coherence for unnatural parity exchanges which are in fact used (likewise for the spin coherence). Absorption should disturb the Regge phases for Reggeized OPE differently in the various amplitudes and also add in  $A_2$  cut effects. Since the absorptive cut associated with the nucleon non-flip  $A_2$  exchange (net helicity flip  $n = 1$ ) pole term is a small correction to an already small amplitude, it follows that spin coherence is a very good approximation for the unnatural parity exchange amplitudes.

In order to calibrate our method against absorbed Regge orthodoxy, we generated intensity components from a strongly absorbed mixture of Reggeized  $\pi$  and  $A_2$  exchange chosen roughly to resemble the data<sup>18)</sup>, and applied our TIAA to the resulting theoretical "data". The results are shown in Fig. 9 -  $\hat{F}^{(0)}$ ,  $\hat{F}^{(-)}$ ,  $\hat{F}^{(+)}$  and  $\hat{F}^{(0)}$  denote the quantities inferred on our method and  $\text{Re } F^{(0)}$ ,  $\text{Im } F^{(0)}$ , etc., are the input amplitudes all plotted against  $\sqrt{-t}$ . The quantities  $\cos \Delta_0$ ,  $\cos \Delta_1$  of Eqs. (5) and (6) came out to lie between 1.0 and 0.92 (a smaller spread than the typical error bar in Fig. 5) up to and including  $\sqrt{-t} = 2.5 \mu$ . The corresponding phase difference between  $F^{(0)}$  and  $-F^{(-)}$  varies from  $3^0$  to  $23^0$ . This "experiment" suggests firstly that our method may well give a reasonable determination of the moduli

of the production amplitudes ; secondly, it illustrates the insensitivity of the constraints to quite appreciable breakdowns of phase coherence at the present level of experimental statistical accuracy.

The amount of transverse rho production at  $t = 0$  sheds an interesting light on absorbed Reggeism. The essence of OPEA at high energies is expressed in the following equation for the net helicity flip zero ( $n = 0$ ) amplitude

OPEA Williams Model (OPEK)

$$S_{+-}^{(1)} = S_{\text{abs}} \otimes \frac{\sqrt{2} t}{t - \mu^2} \Phi(t) \longrightarrow \frac{\sqrt{2} \mu^2}{t - \mu^2} \Phi_W(t) \quad (11)$$

Here the quantity  $\Phi(t)$  represents all additional factors - coupling constants, form factors including all Regge factors aside from the dependences explicitly shown. If  $\Phi(t)$  is a constant, then the substitution shown in the last part of Eq. (11) consists in the removal of major  $J = \frac{1}{2}$  contributions to production <sup>4)</sup>

and can plausibly be attributed to strong central absorption. The procedure can also be adopted even when  $\Phi(t)$  is not a constant, for example for Reggeized OPE. Fox <sup>19)</sup> has dubbed this general recipe "Poor Man's Absorption" (PMA) and has discussed its implications <sup>20)</sup>. We have applied this prescription (PMA) to the pion Regge pole input used in the strong absorption model (SCRAM) test for our analysis method (Fig. 9). The crucial characteristic of the OPE input is an exponential collimation factor

$\Phi(t) = \exp(0.04t/\mu^2)$  chosen to mimic conventional Regge collimation effects. The crucial output is the  $t = 0$  intercept which is related to the value of the parameter <sup>15)</sup>  $\gamma_1^P$

$[S_{+-}^{(1)}(t=0) = \sqrt{2} \gamma_1^P$  in the normalization where

$\Phi(t=0) = \bar{1}$ . With the conventional form factors the "Poor Man's Cut" is much larger than the "Rich Man's Cut" (SCRAM  $\pi$  cut) <sup>21)</sup>.



Furthermore it is of the correct magnitude to explain the entire observed effect from  $p_{\text{lab}} = 2.7$  to  $15 \text{ GeV}/c$  [see Fig. 10, which is an up-dated version of Fig. 1 of Ref. 15]. In contrast, the orthodox absorbed Regge approach has a substantial contribution from absorbed  $A_2$  exchange to reinforce the contribution from absorbed  $\pi^-$  exchange. The detailed differences between the predictions from these two approaches need careful study. The outcomes are likely not so sharply contrasting as might at first sight appear - for example the relative energy dependence of the  $\pi$  and  $A_2$  contribution on the absorption model will go as  $s^{\alpha_{\pi}(\bar{t})} \approx s^{\alpha_{A_2}(\bar{t}_{A_2})}$  not as  $s^{\alpha_{\pi(0)} - \alpha_{A_2(0)}}$  where  $\bar{t}_{\pi}(\bar{t}_{A_2})$  is the average  $t$  value sampled by the convolution <sup>22)</sup>. Mass dependence does not distinguish between these alternatives. Photoproduction at small  $t$  is readily accommodated in both frameworks <sup>23), 24)</sup>.

We have seen that, although compatible with the small  $t$  ( $|t| < 10 \mu^2$ ) data, the model assumptions used in our amplitude analysis are not stringently tested and sizeable breakdowns of phase coherence by  $\sim 20^\circ - 30^\circ$ , as possible in the SCRAM model, cannot be ruled out. Data of increased statistical precision will further tie down the production amplitudes. In particular the density matrix element  $\rho_{1-1}^H$ , being governed by product of amplitudes  $S^{(1)}$  and  $S^{(-1)}$ , i.e., the product of the no net flip and double flip amplitudes (assuming predominant nucleon flip), is an especially informative quantity. It is also of great interest to extend the study of the production amplitudes to larger  $|t|$  values. The behaviour of  $\rho_{00}^H(d\sigma/dt)$  and S wave dipion production near  $t = -0.6 \text{ GeV}^2$  is of particular interest. As pointed out by Fox <sup>20)</sup>, the underlying unnatural parity exchange is presumably nucleon helicity flip and corresponds to an "unhappy" net flip  $n = 1$  amplitude - i.e., the expected absorption zero in  $\text{Im } F^{(0)}$  does not coincide with a wrong signature nonsense zero ( $\alpha_{\pi} = -1$ ). In addition to detailed  $t$  dependence, it will be interesting to peruse  $M_{\pi\pi}$  and dipion spin dependence. The Williams model has analogous predictions for D wave production with the predominant background again in  $m = 1$  helicity states.

However, substantial progress towards the goal of a complete amplitude analysis must await production experiments on polarized targets<sup>2),25)</sup>. Dipion production is a very attractive field for such work. With the predominant exchanges already in part understood and potentially complete measurements in prospect, a big advance in our understanding can be looked for. A start has been made by Sonderegger and Bonamy<sup>11)</sup> with measurements on  $\pi^-p(\uparrow) \rightarrow \pi^0\pi^0n$ . They report a considerable asymmetry indicative of  $A_1$  exchange, which is an important experimental result to be checked. A substantial  $A_1$  coupling<sup>26)</sup> would of course disrupt the spin coherence assumption but, as in the case of phase coherence, a sizeable breaking could pass unnoticed. One can even devise special, but by no means implausible, coupling schemes for  $A_1$  to  $\int \pi$  and  $\varepsilon \pi$  such that there is no breaking of spin coherence - this requires the ratio of nucleon helicity non-flip to flip to be independent of the dipion helicity state. Polarization experiments on  $\pi^-p \rightarrow \pi^+\pi^-n$  will be of the greatest interest, allowing us to settle these points and many others.

#### ACKNOWLEDGEMENTS

We thank Gordy Kane, Robert Worden and members of the CERN-Munich group, especially Walter Blum, Bernard Hyams and Wolfgang Ochs, for very useful conversations.

ANALYSIS	$c^{(0)}$	$c$	$c_s^{(0)}$	$D^{(0)}$	$D^{(-)}$	$D^{(+)}$	$D_s^{(0)}$	$\cos \Delta$	$\chi^2/\text{NDF}$	$\gamma_1^P$	$c_s^{(0)}/c^{(0)}$
40 Fit to t channel data	34.2	- 9.34	12.78	-0.091	-0.106	-0.071	-0.092	0.997	1.65	0.90	0.374
60 Fit to t channel data	34.3	- 9.25	12.88	-0.092	-0.104	-0.069	-0.096	1.000	1.46	0.89	0.375
40 Fit to s channel data	34.10	- 8.61	14.69	-0.086	-0.094	-0.074	-0.101	0.883	1.53	0.82	0.431
For comparison SLAC fit by Williams model Ref. 4)	38.5	-10.7	14.3	-0.098				1.000			

TABLE : Parameters from representative t dependent amplitude analyses  
[cf. Eqs. (7) to (10)].

## REFERENCES

- 1) F. Bulos et al. - Phys.Rev.Letters 26, 1453 (1971).
- 2) The case of pure vector meson production is discussed in :  
G.C. Fox - Invited Talk at the Second International  
Conference on Polarization and Polarized Targets,  
Berkeley (1971), Preprint CALT-68-334.
- 3) The related process  $\pi^- p \rightarrow K^* \Lambda$  is discussed by A.D. Martin  
at this Rencontre.
- 4) P.K. Williams - Phys.Rev. 181 (1963) ; D1, 1312 (1970).
- 5) J.H. Scharenguivel et al. - Phys.Rev.Letters 24, 332 (1970).
- 6) A parallel investigation is being pursued by Ochs (W. Ochs,  
private communication).
- 7) P. Baillon et al. - Phys.Letters 35B, 453 (1971) [fit to  
data of Ref. 1].
- 8) However, we do not include a 12% nucleon non-flip contamina-  
tion from  $\pi^- p \rightarrow \pi^+ \pi^- \Delta^0$  as is done in Ref. 7).  
Among other things this contamination may distort  
density matrix elements at small  $t$ .
- 9) G.V. Dass and C.D. Froggatt - Nuclear Phys. B8, 661 (1968).
- 10) Saturation of standard Schwarz inequalities has been tested  
against density matrix elements from Ref. 1) by :  
J.J. Sakurai - Lectures delivered at International  
School of Subnuclear Physics, Erice, Sicily (1971),  
Preprint UCLA/71/TEP/39.

- 11) P. Sonderegger and P. Bonamy - Presented at Lund Conference (1969) ;  
P. Sonderegger - "High Energy Collisions", Third International Conference on High Energy Physics, Stony Brook (1969), Gordon and Breach, New York.
- 12) E.I. Shibata, D.H. Frisch and M.A. Wahlig - Phys.Rev.Letters 25, 1227 (1970).
- 13) In the plot of  $\text{Re } \mathcal{F}_{10}^J$  in Fig. 8a, the two dashed curves indicate the change made by allowing for the correct non-zero value of  $\sqrt{-t_{\min}} = 0.14 \mu$ .
- 14) CERN-Munich Group - Private communication.
- 15) C.D. Froggatt and D. Morgan - Phys.Letters 33B, 582 (1970).
- 16) P.E. Schlein - Phys.Rev.Letters 19, 1052 (1967).
- 17) E. Malamud and P.E. Schlein - Phys.Rev.Letters 19, 1056 (1967).
- 18) We did not attempt to make a "best fit" to the data and we neglected the nucleon non-flip  $A_2$  exchange amplitude, which is inessential for the purposes of our discussion.
- 19) G.C. Fox - "High Energy Collisions", Third International Conference on High Energy Physics, Stony Brook (1969), Gordon and Breach, New York.
- 20) G.C. Fox - "Phenomenology in Particle Physics, 1971", Proceedings of Conference held at the California Institute of Technology (March 1971).

- 21) More details on the amplitude as a function of  $t$  and also in impact parameter space are given in :  
C.D. Froggatt and D. Morgan - Contribution to Fourth International Conference on High Energy Collisions, Oxford (April 1972). See also Ref. 20).
- 22) This was emphasized to us by G.L. Kane (private communication).
- 23) C.F. Cho and J.J. Sakurai- Phys.Letters 30B, 119 (1968) ; Phys.Rev. D2, 517 (1970).
- 24) R.P. Worden - Nuclear Phys. B37, 253 (1972).
- 25) D. Morgan, G.C. Oades, R.J.N. Phillips and G.A. Ringland - "A Case for Medium Energy Hadron Physics", p. 14, Rutherford Laboratory Memorandum RHEL/M/C8 (June 1971).
- 26) Evidence for a sizeable isoscalar unnatural parity exchange contribution to  $\pi^{\pm}_p \rightarrow \rho^{\pm}_p$  (i.e., H meson type) at 2.7 GeV/c is presented by G. Gidal at this Rencontre.
- 27) L.D. Jacobs - Saclay Preprint (1971), submitted to Phys.Rev.

## FIGURE CAPTIONS

- Figure 1 Plot of  $t$  channel  $m = 0$  P wave production amplitude  $F^{(0)}$  : derived by TDAA [Eqs. (7)-(10) 6C Fit] (full line) ; TIAA (points with error bars) ; and, for comparison the fit of Ref. 7) using the Williams model. (Note : the points with error bars are not data.)
- Figure 2 Plot of  $t$  channel, unnatural parity exchange transverse P wave production amplitude  $F^{(-)}$ . Legend as for Fig. 1.
- Figure 3 Plot of  $t$  channel, natural parity exchange transverse P wave production amplitude  $F^{(+)}$ . Legend as for Fig. 1.
- Figure 4 Plot of S wave production amplitude  $F_s^{(0)}$ . Legend as for Fig. 1.
- Figure 5 Results for the constraint testing quantities  $\cos\Delta_0$ ,  $\cos\Delta_1$  [Eqs. (5) and (6)] for the  $t$  channel TIAA.
- Figure 6 Plot of s channel, natural and unnatural parity exchange transverse P wave production amplitudes  $F^{(+)}$  and  $F^{(-)}$ . Legend as for Fig. 1.
- Figure 7 Example of TDAA fit to  $d\sigma/dt$  (units  $\mu\text{b}/\text{GeV}^2$ ) (6C  $t$  channel Fit).
- Figure 8 TDAA fits to density matrix elements :
- $t$  channel 6C Fit ;
  - s channel 4C Fit.

Figure 9 Test using theoretical "data" (SCRAM  $\pi + A_2$ ) of analysis method based on assumption of spin and phase coherence.  $\text{Re } F^{(0)}$ ,  $\text{Im } F^{(0)}$ , etc., are the input amplitudes (full lines) ;  $\hat{F}^{(0)}$ , etc., (dashed lines) is the TIAA output.

Figure 10 Estimates of the parameter  $\gamma_1^P$  (a measure of the amount of transverse rho production at  $t = 0$  relative to the OPE signal) as a function of  $p_{\text{lab}}$ . Up-dated version of Fig. 1 from Ref. 5). The two extra points are from Jacobs' new determination for  $p_{\text{lab}} = 2.77 \text{ GeV}/c$  ( $\Phi$ ) and the present determination for  $p_{\text{lab}} = 15 \text{ GeV}/c$  ( $\Phi$ ) [we have provisionally assigned a notional span  $\gamma_1^P = 0.90 \pm 0.08$  on the basis of the fits shown in the Table and the  $\gamma_1^P = 1$  fit of Ref. 7]. The curves relate to theoretical predictions [OPEK, Ref. 4), CS, Ref. 23], discussed in the text and in Ref. 15).



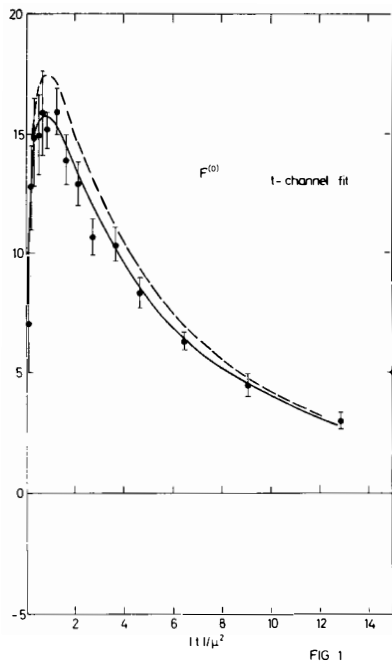


FIG 1

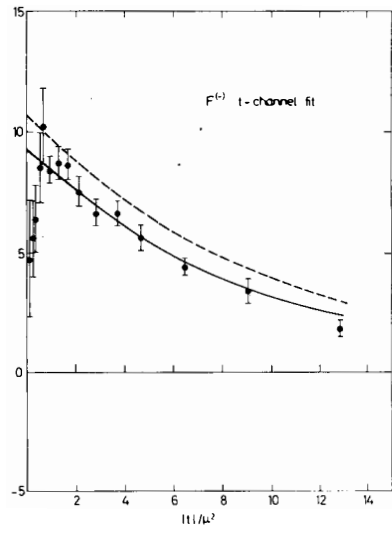


FIG 2

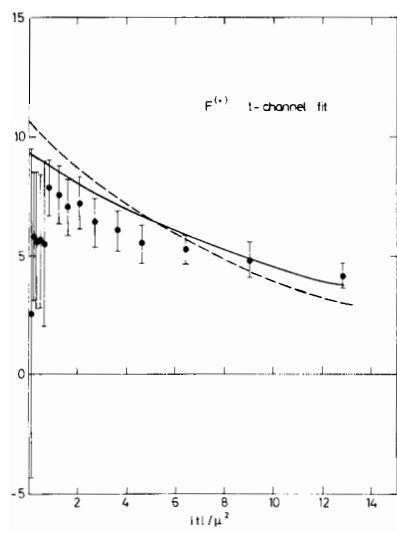


FIG 3

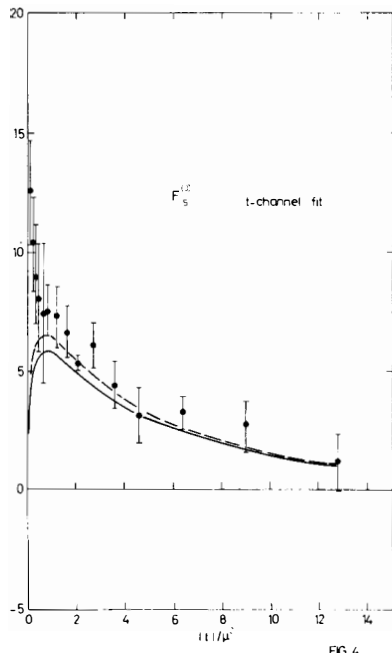


FIG 4

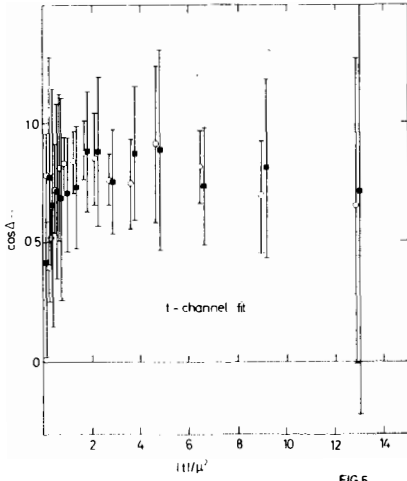


FIG 5

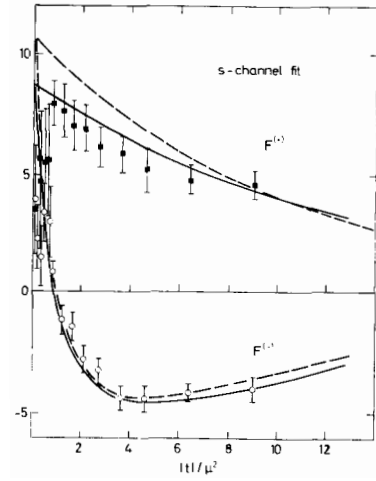


FIG 6

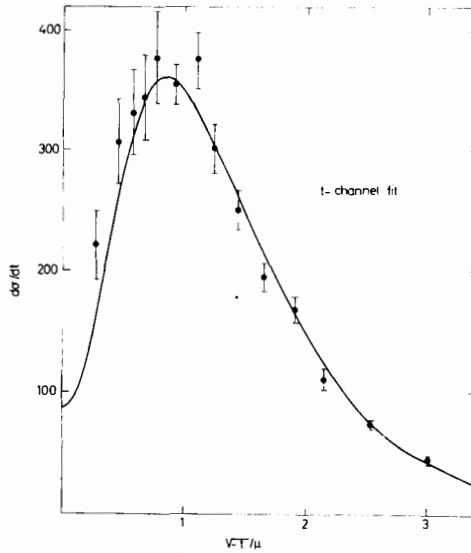


FIG 7

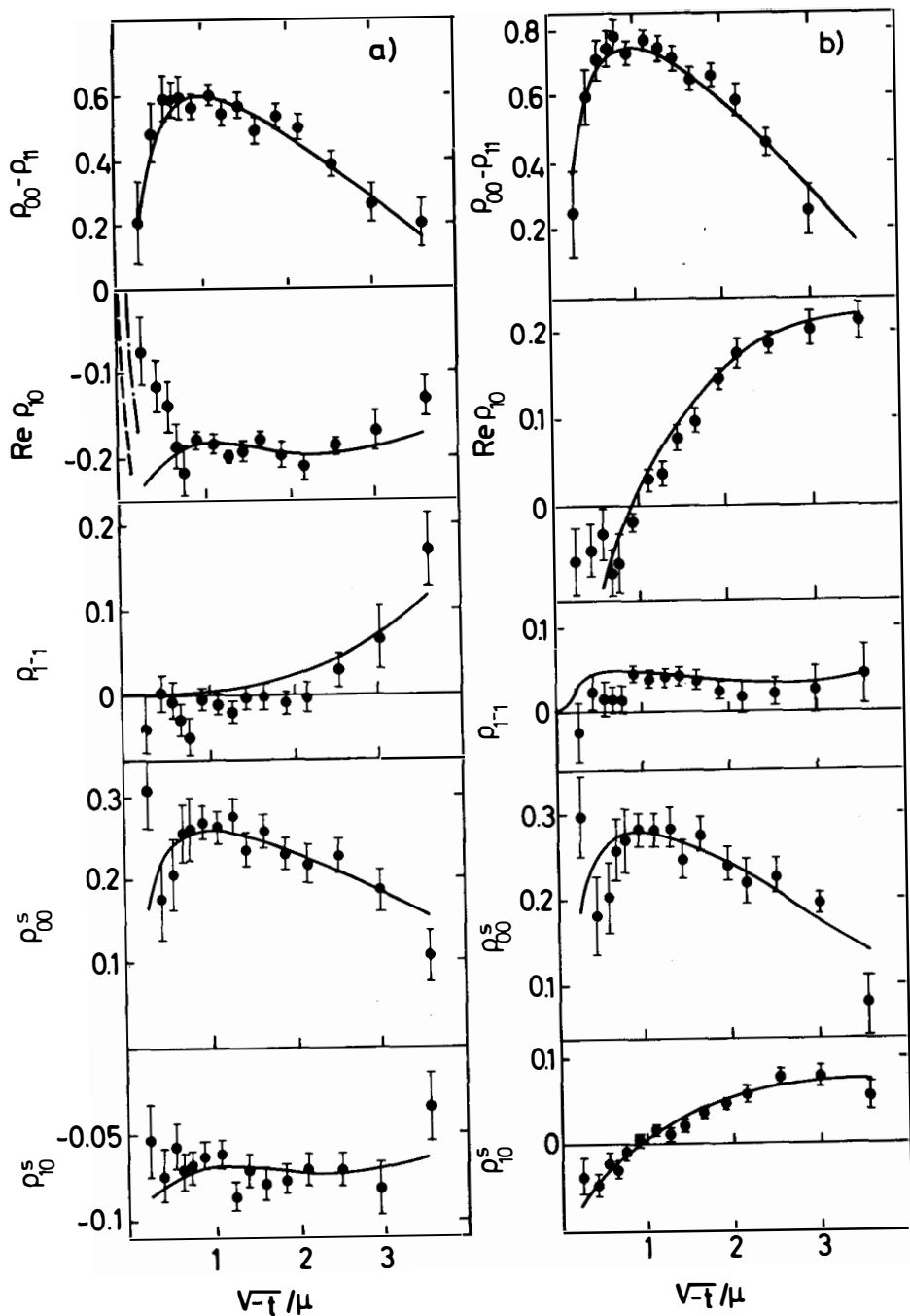
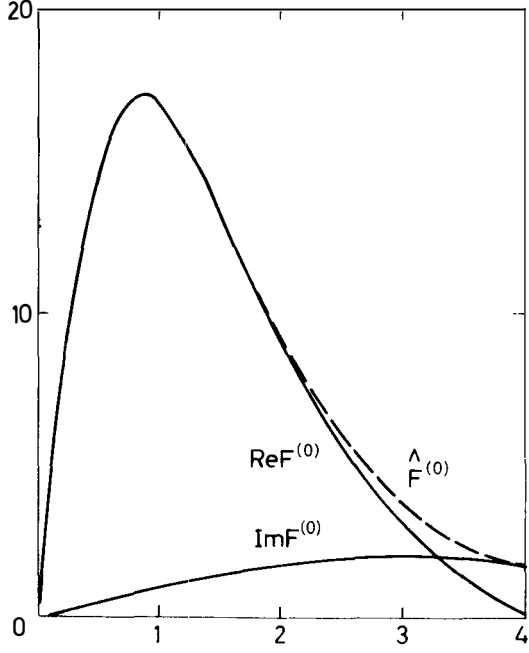
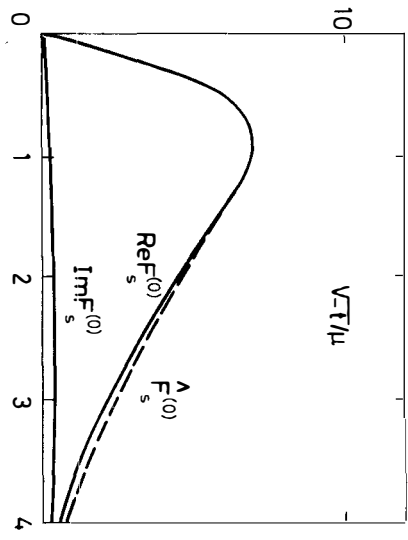
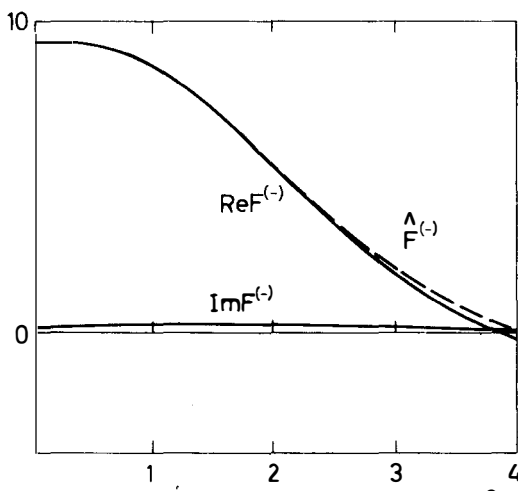
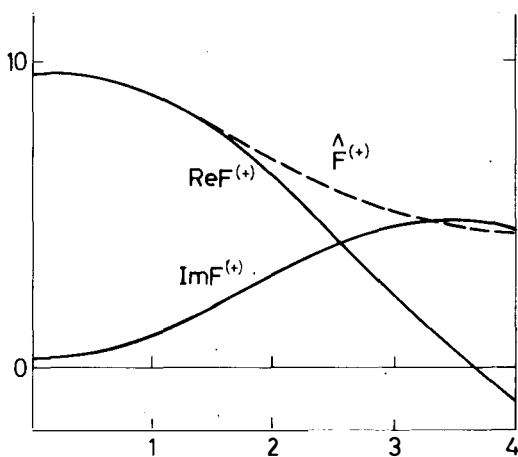


FIG. 8



$V-T/\mu$  FIG.9

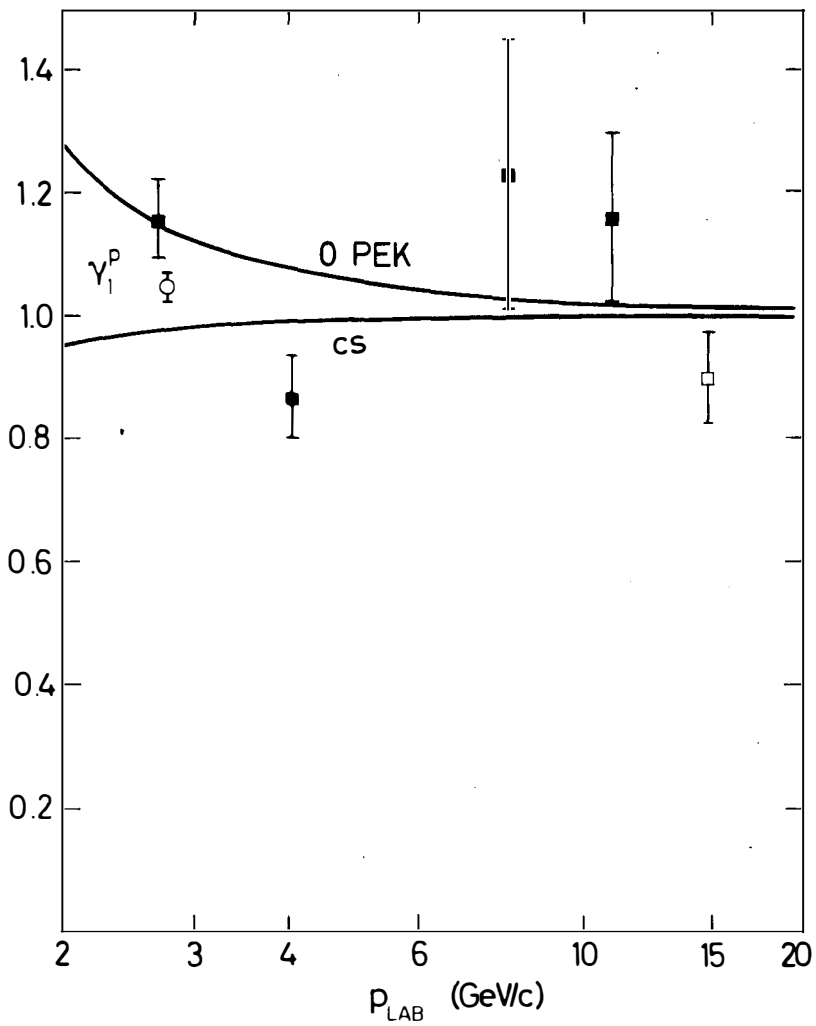


FIG.10